

HydroCube Mission Concept: P-Band Signals of Opportunity for Remote Sensing of Snow and Root Zone Soil Moisture

Simon Yueh*^a, Rashmi Shaha, Xiaolan Xua, Kelly Elder^b, Chun Sik Chae^a, Steve Margulis^c, Glen Liston^d, Michael Durand^e, and Chris Derksen^f

^aJet Propulsion Laboratory, California Institute of Technology, California, USA

^bUnited States Forest Service, Fort Collins, Colorado, USA

^cUniversity of California at Los Angeles, California, USA

^dColorado State University, Fort Collins, USA

^eOhio State University, Columbus, Ohio, USA

^fEnvironment and Climate Change Canada, Canada

ABSTRACT

We have developed the HydroCube mission concept with a constellation of small satellites to remotely sense Snow Water Equivalent (SWE) and Root Zone Soil Moisture (RZSM). The HydroCube satellites would operate at sun-synchronous 3-day repeat polar orbits with a spatial resolution of about 1-3 Km. The mission goals would be to improve the estimation of terrestrial water storage and weather forecasts. Root-zone soil moisture and snow water storage in land are critical parameters of the water cycle. The HydroCube Signals of Opportunity (SoOp) concept utilizes passive receivers to detect the reflection of strong existing P-band radio signals from geostationary Mobile Use Objective System (MUOS) communication satellites. The SWE remote sensing measurement principle using the P-band SoOp is based on the propagation delay (or phase change) of radio signals through the snowpack. The time delay of the reflected signal due to the snowpack with respect to snow-free conditions is directly proportional to the snowpack SWE. To address the ionospheric delay at P-band frequencies, the signals from both MUOS bands (360-380 MHz and 250-270 MHz) would be used. We have conducted an analysis to trade off the spatial resolution for a space-based sensor and measurement accuracy. Through modeling analysis, we find that the dual-band MUOS signals would allow estimation of soil moisture and surface roughness together. From the two MUOS frequencies at 260 MHz and 370 MHz, we can retrieve the soil moisture from the reflectivity ratio scaled by wavenumbers using the two P-band frequencies for MUOS. A modeling analysis using layered stratified model has been completed to determine the sensitivity requirements of HydroCube measurements. For mission concept demonstration, a field campaign has been conducted at the Fraser Experimental Forest in Colorado since February 2016. The data acquired has provided support to the HydroCube concept.

Keywords: microwave remote sensing, snow, soil moisture, radar, radiometer

INTRODUCTION

Despite their importance, Snow Water Equivalent (SWE) and Root Zone Soil Moisture (RZSM) are arguably two of the least measured hydrologic states in the Earth System. Snow covered area can be relatively easily measured from space using visible/near-infrared sensors (except for heavily forested areas which can mask underlying snow), but such measurements provide no direct information on the mass of snow on the ground. Methods using multi-frequency passive microwave measurement techniques (e.g. [1,2,3]) have a long heritage, but are known to suffer from many problems including, the many-to-one relationship between brightness temperature and SWE, sensitivity to grain size, signal saturation for deeper snow and the high-degree of sub-grid heterogeneity in mountainous environments [4]. With respect to soil moisture, the Soil Moisture Active Passive (SMAP) mission [5] is already providing new insight into near-surface soil moisture storage, but does not provide direct information about RZSM, which plays a key role in the evapotranspiration/latent heat flux to the atmosphere and the modulation of recharge to near-surface groundwater aquifers.

The current state-of-the-art remote sensing method for RZSM is based on the multi-frequency P-/L-band synthetic aperture radar technique [6]; however, the US Department of Defense has recently worked with the International Telecommunication Union (ITU) to designate the US Space Objects Tracking Radar (SOTR) as the primary user of the

435 MHz band. This change will prohibit spaceborne P-band earth remote sensing radars from operating over North America and most of Europe, severely limiting our ability to monitor RZSM. At this point, there are no clearly viable alternative remote sensing methods for RZSM and SWE under canopy.

The HydroCube concept would advance the P-band SoOp technologies for remote sensing of SWE and RZSM to lead to cost effective satellite missions for global sampling. P-band frequencies have the capability to penetrate through heavy vegetation and snow, offering potential new capabilities not achievable by current high frequency (>10 GHz) microwave technologies.

Beyond the demonstration of new SoOp measurement techniques, reliable retrievals of SWE and RZSM would have significant value to hydrologic science and water resources applications. Specifically, both SWE and RZSM contribute directly to the partitioning of precipitation into runoff and infiltration (and subsequent recharge), often in a coupled way. Seasonal snowpacks act as a large virtual reservoir in many mid-latitude regions [7] that delay the onset of infiltration and runoff from the time of initial precipitation. The conversion of SWE to runoff is in part a direct, but nonlinear, function of snowmelt rates (higher snowmelt rates will generally lead to more runoff). Being able to monitor SWE accumulation would provide a key constraint on how much *potential* runoff could occur during Spring ablation and the ability to monitor SWE disappearance rates would provide a key constraint on how much SWE is *actually* partitioned into runoff vs. infiltration/recharge. Moreover, the conversion of SWE to runoff is directly coupled to the RZSM state underlying the snowpack. Saturated or frozen soils will further increase the conversion of snowmelt to runoff and being able to monitor both would provide a significant leap forward in our ability to predict floods. For spring streamflow forecasts in the Western U.S., [8] demonstrated that knowledge of early-spring SWE generally contributes most to streamflow forecast skill, with early-spring soil moisture often also playing a significant role. In other seasons, soil moisture has been found to dominate forecast skill with potential to contribute skill at lead times up to 6 months [9].

P-BAND SIGNALS OF OPPORTUNITY CONCEPT

Land and ocean remote sensing with Signals of Opportunity, such as Global Navigation Satellite System (GNSS) reflectometry (GNSS-R), has been developed substantially over the last 15 years, culminating in the selection of the CYGNSS tropical storm observation mission by NASA [10]. The use of GNSS signals at L-band (1.2 and 1.5 GHz) for surface soil moisture retrieval has been demonstrated by airborne measurements during the Soil Moisture Experiment 2002 [11] and a field campaign in Europe [12], and its theoretical principle is based on the response of L-band microwave reflectivity to surface soil moisture [13]. Navigation (GNSS) signals were well matched for reflectometry, due to their use of pseudorandom noise (PRN) codes for ranging. GNSS signals, however, have a few significant disadvantages, particularly for application to land remote sensing including: very low signal power, a spectrum allocation restricted to L-band, and limited penetration into soil and forest canopies. An alternative is to use high transmitting power satellite communication signals [14]. The high economic value of satellite communications would drive the evolution of satellite service providers to use all available spectrum in the most efficient manner possible, assuring the availability of SoOp illumination sources in nearly all microwave bands penetrating the Earth's atmosphere.

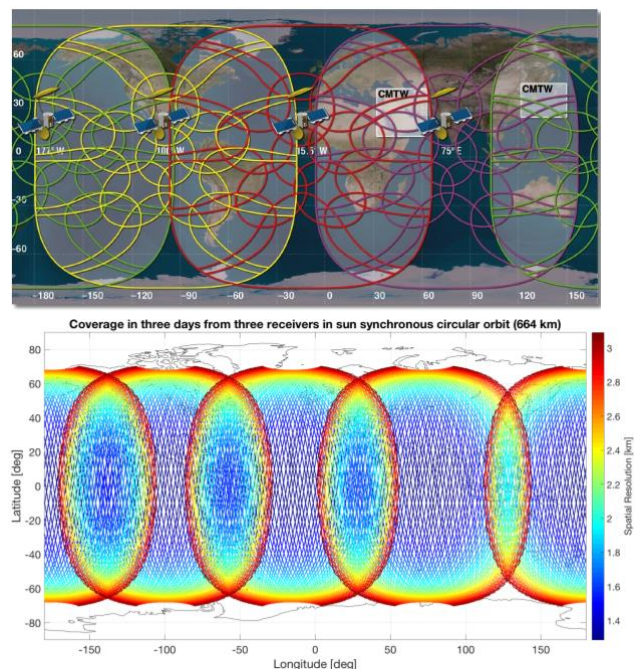


Figure 1. Global coverage of 4 MUOS satellites in geostationary orbits (top). The sampling coverage by three SoOp Cube-satellites operating at sun-synchronous orbits with 3-day repeat.

The particular P-band communication satellites of interests to the HydroCube concept are the Navy's Mobile Users Objective System (MUOS) operating at P-band frequencies [15]. There are four MUOS satellites at geostationary altitudes, providing global coverage, except near the polar cap (Fig. 1). Each satellite broadcasts dual-frequency channels at P-band (360-380 MHz and 240 -270 MHz). The transmit power in terms of power density on the ground is significantly stronger than GNSS, thus allowing small SoOp satellite receivers operating at low earth orbit to capture reflection with a high signal to noise ratio. In terms of potential sampling, the bottom panel in Fig 1 shows the coverage map corresponding to three hypothetical Cubesats (~10cmx20cmx60cm in volume) with P-band SoOp receivers. Such a configuration would allow global sampling every three days with track spacing of 50 km or smaller at a spatial resolution of 1-3 km. Tripling the number of SoOp receivers would reduce the track spacing to about 10 km. It is important to note that a key feature of such a P-band SoOp platform would be a discontinuous (i.e. non-imaging) sampling pattern (Fig. 1), whereby repeat retrievals would be available along-track, but with gaps in spatial coverage. While such a retrieval dataset would still provide an unprecedented new picture of the evolution of SWE and RZSM at large scales, a key aspect of the Hydrocube concept is to demonstrate, via OSSEs, how a space-time continuous estimates of SWE, RZSM, and other hydrologic states and fluxes (e.g. runoff and evapotranspiration) would be possible using the new retrievals of SWE and RZSM in a data assimilation framework.

PHYSICAL BASIS OF RZSM AND SWE ALGORITHM USING SOOP

With the breakthrough demonstrations that reflectometry can be performed using any sufficiently random digital signal, with sufficient power, this proposed HydroCube concept has the potential to produce the seminal work defining P-band SoOp reflectometry as an entirely new technique for microwave remote sensing of RZSM and SWE, alongside the well-established fields of active radar and passive radiometry.

Dry snow

The P-band SoOp measurement principle uses repeat pass data to exploit the change of coherent phase for radio propagation through dry snowpack [16,17] and has been demonstrated by experimental data in [18]. The amplitude and phase of the detected SoOp signal contain information on the amount of water stored in the snowpack and soil. For a layered stratified medium depicted in Fig. 2, the radio signal reflected by the lower interface can be characterized as

$$E = \text{Re} \left[\frac{i^{2\pi(r_1+r_2)}}{\lambda} e^{-\alpha} e^{i\phi_s} \right] \quad (1)$$

Here R is the reflection coefficient, and is mostly related to the soil moisture in the bottom layer. The second term represents the total phase change due to the distance between the satellites and ground (r_1+r_2). The third term represents the attenuation by the vegetation or snow layer above the soil. The phase angle in the last term is due to the radio propagation through the snowpack or vegetation.

The phase change due to the snowpack is related to the snow depth (d) by

$$\phi_s = \frac{4\pi}{\lambda} d \left[\text{Re}(\sqrt{\epsilon - \sin^2\theta}) - \cos\theta \right] \quad (2)$$

where θ is the incidence angle, λ is the wavelength, and ϵ is the dielectric constant of snow. "Re" is a function, taking the real part of its argument.

The dielectric constant (ϵ) of dry snow can be related to the snow density (ρ) of up to 0.4 g/cm³ by [19,20]

$$\epsilon = 1 + 1.6\rho + 1.86\rho^3 \quad (3)$$

For low incidence angles and small snow density, ϕ_s can be approximated by [21,22]

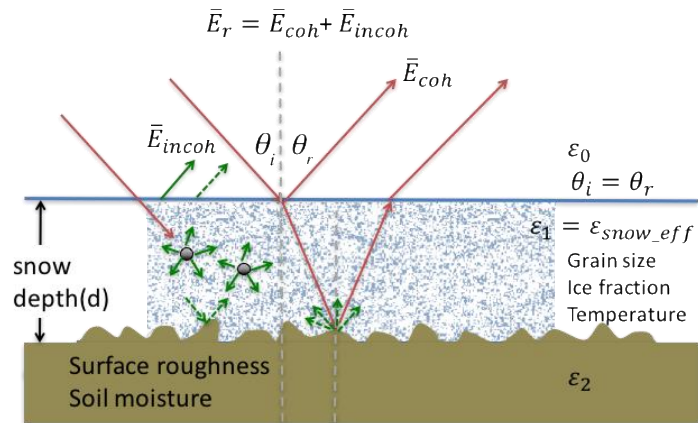


Figure 2. Physical principle of SoOp modeled by stratified medium. The reflected signal consists of coherent and incoherent electric fields, characterized by E_{coh} and E_{incoh} .

$$\phi_s = \frac{4\pi \cdot 0.8d\rho}{\lambda \cos\theta} = \frac{4\pi \cdot 0.8SWE}{\lambda \cos\theta} \quad (4)$$

Therefore, the phase change is approximately linearly related to the SWE of dry snowpack. More rigorous simulation based on stratified medium model [23,24] has demonstrated the linear relationship for a snow density of 0-0.4 g/cm³.

This suggests we can use SoOp (bistatic) repeat pass phase detection to detect the phase change caused by the change of SWE (accumulation or depletion). This measurement principle has been demonstrated using field campaign data acquired in 2016 at Fraser Colorado [18]. The test site from which data was acquired in early 2016 has no tree cover, just natural ground with rough surface and residual vegetation debris. The unwrapped phase time series was computed from data collected daily between 5 AM and 6 AM MST between Jan. 16, 2016 and March 11, 2016. There was a high correlation between phase change and SWE (0.94), covering several snowfall and melt/refreeze cycles, while a lower correlation was found between phase change and snow depth (0.69). The root mean square error (RMSE) of the linear regression of retrieved SWE and *in situ* SWE was found to be 7.5 mm [18].

Other Snow Parameters: Stratigraphy, Snow Grain and Density Effects

We have completed a more rigorous modeling analysis based on the stratified medium model (Tsang et al., 1985) to examine the effects of snow stratigraphy, leading to multiple internal reflections between snow layers. The dielectric constant of each layer is computed using the Microwave Emission Model of Layered Snowpacks (MEMLS) described in [20]. The phase angles of reflection coefficients for right-hand circularly polarized transmit and left-hand circularly polarized reflection are illustrated in Fig. 3 for the profile acquired on March 5, 2015. We also computed the average snow density for each snowpack to generate the corresponding reflection coefficient for the single-layer approximation. Computations were completed for P- and L-bands. There is essentially no difference between the results from multi-layered and single-layer approximations. Based on 11 snow density profiles from snow pit measurements acquired in Fraser Colorado in 2015, we find the impact of stratigraphy on the phase change (or path delay) of the reflected signals to be very small.

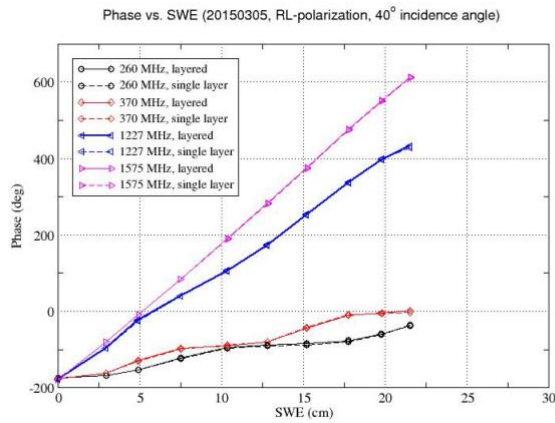


Figure 3. Negligible differences between phase change computed using single- (dashed curves) and multi-layered (solid curves) reflection models at MUOS and GNSS frequencies for the snow density profile acquired on March 5, 2015 at Fraser Colorado.

We have also investigated the impact of snow grain size and density based on the Dense Medium Radiative Transfer (DMRT) model [23]. The conclusion is that the impact of grain size and density are essentially negligible because the grain size of snow is much smaller than the wavelength (~1 m) of P-band frequencies [16,17].

The negligible impact of many snow parameters, that are confounding factors in other methods, is a distinct feature for P-band SoOp reflectometry, a significant algorithm advantage over traditional high frequency (>10 GHz) radar and radiometer techniques, which need to account for layering, grain size and density effects to enable accurate modeling of radar backscatter or microwave emissions.

Wet Snow

We have applied the stratified medium model to examine the effects of wet snow. The dielectric constant of wet snow is characterized by wetness as well as temperature and density [20]. We find that the dielectric constant of wet snow essentially does not change in the frequency range of 260 MHz-1GHz, indicating that the snowpack is essentially non-dispersive in this range of frequencies. The imaginary parts remain quite small from moist to very wet (3-15%). As the snow wetness increases, the dielectric contrast between ground and snow reduces, leading to a reduction in reflection

between the snow and ground interface. In contrast, the dielectric contrast between air and snow increases with wetness. When the wetness reaches above 5%, the total reflection will be dominated by the reflection from the air-snow interface.

The changing dominance of air-snow and snow-ground interfaces leads to the changing correlation of reflected signal with SWE or snow depth. When the snow becomes considerably wet (>5%), the phase change of reflected signal will reduce with increasing snow depth because the air-snow interface will move toward the receiver, thus reducing the path delay (Fig. 4). In this case, the phase angle is related to the snow depth or SWE by

$$\phi_s = -\frac{4\pi}{\lambda} d \cos\theta = -\frac{24}{\rho} f \cos\theta \cdot SWE \quad (5)$$

where “ f ” is in GHz. Hence, for wet snow, the SoOp reflectometer will perform like an altimeter, being most sensitive to the depth of snowpack for wet snow. If the bulk snow density (ρ) is known, the phase angle in degrees for wet snow can be related to SWE. Moreover, in a data assimilation context, prior information from the land surface snow model about snow wetness (and density) can be used to estimate whether the retrieved quantity to be assimilated is SWE or snow depth. In particular, the data assimilation framework, as an enabling component of the overall estimation system, will play a key role in maximizing the retrieval information to tease out the SWE vs. snow depth signal.

SWE Retrieval Under Canopy

We have conducted a preliminary theoretical analysis to estimate the impact of trees on phase change (or path delay) at P-band frequencies. The dielectric constant of vegetation includes the contribution by dry vegetation materials and water content. The dielectric constant of dry materials is about 1.5-2, close to dry snow and essentially does not change over time. The vegetation water content has a direct impact on the dielectric constant, and hence the propagation delay or phase of reflected signal. However, the fractional volume of vegetation is small; the effective dielectric constant (ϵ) of the canopy, a mixture of vegetation material and air, is related to the water content in the canopy (Chukhlantsev et al., 2003), leading to a small perturbation:

$$\epsilon \approx 1 + \Delta\epsilon \quad (6)$$

It was shown in [24] (in their Table 4) that the dielectric constant of coniferous forest is in the range of 1.001 to 1.003, and that of deciduous trees is in the range of 1.003 to 1.2.

The phase change due to the change of dielectric constant for the vegetation thickness (h) can be approximated by

$$\Delta\phi_s \approx \frac{2\pi}{\lambda} h \cos\theta \Delta\epsilon \quad (7)$$

For $\theta = 40^\circ$ and $h = 15\lambda$, the phase change will be about 4 degrees for an increment of $\Delta\epsilon$ by 0.001. Note that λ is 1.15 m at 260 MHz, and thus $h = 15\lambda$ will correspond to a tree height of about 17 m. For a change of $\Delta\epsilon$ from 0.001 to 0.003, the phase change will rise from 4 to 12 degrees, which correspond to about 1 cm in SWE based on the SWE-phase relationship [15,16]. A change of a few degrees has a small impact on SWE retrieval; however, a much larger change will need to be accounted for at P-band frequencies (Fig. 4).

SoOp Measurement Principle for RZSM

The P-band MUOS frequencies allow a penetration of ~0.5-1 m into the soil to sense the change of moisture in the root zone. The P-band frequencies complement the L-band frequencies for the Soil Moisture Active Passive (SMAP) and CYGNSS missions, which are primarily sensitive to the soil moisture in the top few centimeters of soil. We have carried out a modeling analysis based on the stratified medium model. The dielectric constant of the soil is evaluated using the Mironov model [25]. The reflectivity at the MUOS and GNSS frequencies show varying degrees of sensitivity to the soil

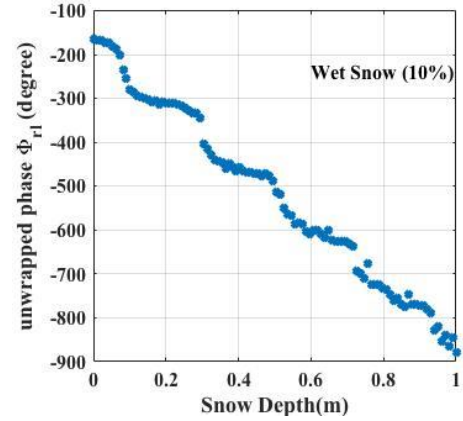


Figure 4. Phase change is related to snow depth for very wet snow where the air-snow interface dominates the coherent reflection. MEMLS snow dielectric model is used for the dielectric constant of snow with wetness. Results correspond to frozen ground and random snow density between 200-300 kg/m³.

moisture at the depth of 50 cm (Fig. 5) based on the exponential vertical profile of soil moisture between the surface and depth of D_n :

$$SM(z) = SM_0 + (SM_{D_n} - SM_0)(e^{-\beta z} - 1)/(e^{-\beta D_n} - 1) \quad (8)$$

Through theoretical modeling analysis, we find that the dual-band MUOS signals together with the CYGNSS L-band reflectivity data can allow estimation of soil moisture profile. We have developed a retrieval algorithm by a minimization of the sum of squared differences between simulated and modeled reflectivity at three frequencies, two for MUOS and one for GNSS:

$$Cost\ Function = \sum_{i=1}^3 \frac{(r_i - r_{model}(SM_0, SM_{D_n}, \beta))^2}{\sigma_i^2} \quad (9)$$

Note that the required ancillary data are the clay content of soil and depth parameter D_n .

We have carried out a Monte Carlo simulation by simulating the reflectivity at MUOS and GNSS frequencies for right-hand circularly polarized transmit and left-hand circularly polarized receive, adding Gaussian random noise based on the estimated Signal-to-Noise ratio, and performing parameter inversion of soil moisture parameters based on the minimization of the cost function.

We can assess the retrieval performance for the complete range of soil moisture parameters and the impact of uncertainties of ancillary data which is illustrated in Fig. 6. Should there be negligible errors in the ancillary data, the retrieved vs. input soil moisture falls on the one-to-one line and the error bars representing the 1 standard deviation of the Monte Carlo simulation are mostly less than 1 percent (Fig. 6, left panel). If the knowledge of clay content is significantly

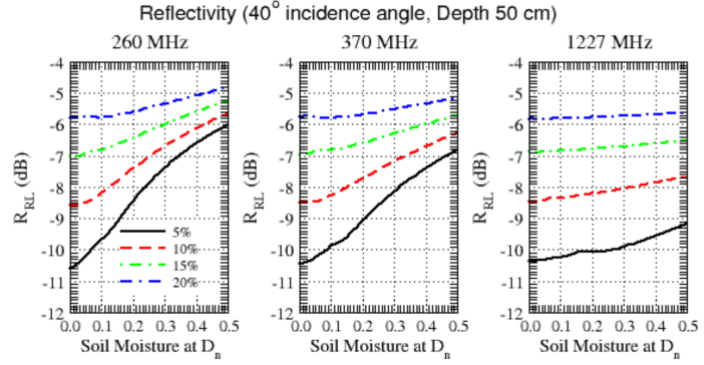


Figure 5. MUOS P-band frequencies (260 and 370 MHz) have a much stronger response to RZSM than GPS frequencies (1227 MHz). A stratified medium model is used for the coherent reflectivity of soil with a vertical moisture profile (exponential profile with 3 parameters). Each panel has four curves, corresponding to four surface soil moisture levels of 5, 10, 15 and 20 percent.

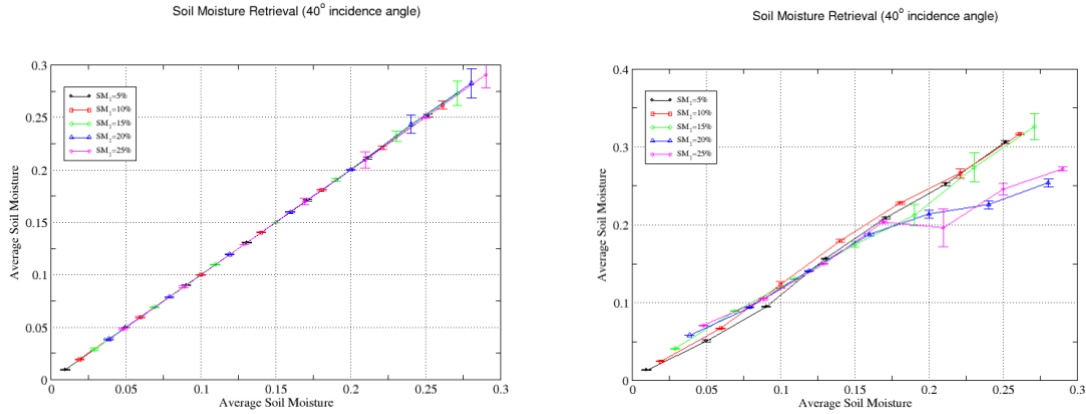


Figure 6. Simulation of soil moisture retrieval error. Simulated reflectivities at 3 frequencies, including 260 MHz, 370 MHz, and 1227 MHz were used to retrieve 3 parameters, SM_1 , SM_t and β with a clay fraction of 20 percent. Gaussian random noise was added to the simulated reflectivity based on the expected signal-to-noise ratio of a spaceborne SoOp. (Left panel) Excellent accuracy is achieved if the ancillary clay content and depth are known. (Right panel) Retrieval bias due to an error in the knowledge of clay content (30 percent) is small for dry soil and larger for wet soil.

biased by 50%, the retrieval uncertainties remain mostly under 2 to 3 percent, except a large bias of about 5 to 10 percent for high RZSM (Fig. 6, right panel). Since clay content is a static parameter, it could be estimated adaptively as part of the data assimilation framework if biases are expected. Overall, the simulations indicate that multi-frequency reflectometry based on MUOS and GNSS has an excellent capability for RZSM retrieval and is quite tolerant to the uncertainty of ancillary inputs.

FIELD EXPERIMENTS AND DATA

We have completed a proof-of-concept experiment alongside an intensive system of *in situ* sensors to validate the SoOp concept at the Fraser Experimental Forest (FEF) Headquarters, near Fraser, Colorado (39.847°N, 105.912°W) during the winter of 2015-2016 (Shah et al., 2017). FEF is a 93 km² research watershed in the heart of the central Rocky Mountains approximately 80 km west of Denver. The FEF Headquarters is operated by the US Forest Service (USFS) with the intent to study watershed hydrology in the subalpine zone. This site maintains long-term records on hydrology, climate, forest structure and growth, and responses to forest management. FEF's favorable location, network of other instrumentation, and long record of climate monitoring made it a well-suited site for this research.



Figure 7. Experimental setup at USFS FEF located at Fraser Colorado: Site A (no vegetation) and Site B (vegetation). Dual-frequency P-band SoOp receivers at each site for data acquisition every three hours.

A flat location at FEF with little forest vegetation was selected in 2015-2016. A 15.2 m tower was erected with P-band antennas, LNAs, and filters installed at the top. One additional tower was deployed in summer 2016 to make observations at two locations with different background roughness and vegetation cover. Both of these sites recorded data at MUOS frequencies. The data was recorded every three hours. The new site has some Black Spruce trees with trees up to 3 meters in height (Fig. 7). So, a study on the effect of vegetation on the under-canopy snow measurement can be done with this site.

During the experiments, *in situ* measurements of snow depth and other snowpack properties were performed every one to two weeks for comparison with the remotely sensed data. Snowpack measurements were taken next to the tower site in a location that would not compromise the satellite signal. A network of soil moisture sensors, time-lapse cameras, acoustic depth sensors, and meteorological instruments were installed next to the site to collect *in situ* measurements of snow, weather, and soil conditions. The camera recorded images three times a day (during daytime) and the soil moisture probes, located at 5 cm, 10 cm, 27 cm, and 40 cm, recorded soil moisture and soil temperature at the same interval as that of the reflection data i.e. every three hours.

The phase information from both sites and both frequencies has been computed from data collected at 12 PM UTC between 10/27/2016 to 02/16/2017 using the same procedure described in [18]. Figure 8 shows the phase information that was retrieved. A strong phase correlation was found between sites A and B for

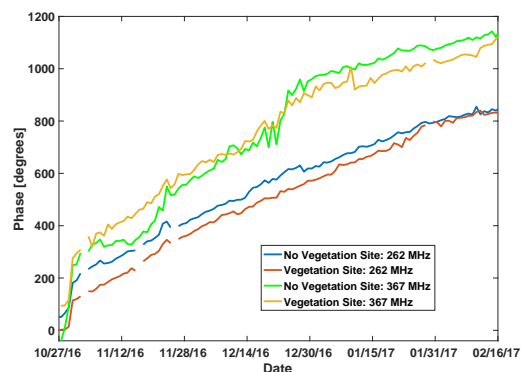


Figure 8. Phase change computed from data collected at 12 PM UTC between 10/27/2016 to 02/16/2017. High correlation (0.96-0.99) was observed between sites and between frequencies.

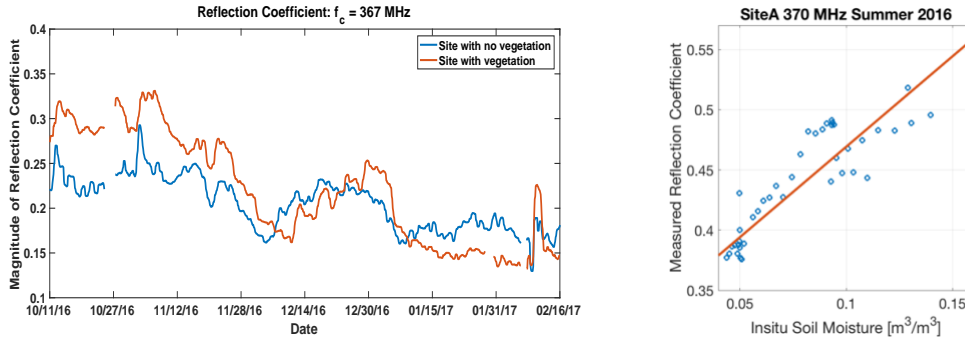


Figure 9. Right panel shows a high correlation (0.87) between the measured reflection coefficient and in situ soil moisture. Left panel shows the comparison between the measured reflection coefficient from two sites (not vegetated and vegetated). A similar trend is observed from both sites.

both 262 MHz (correlation of 0.99) and 367 MHz (correlation of 0.99). In addition, the correlation between the two frequencies was high, 0.96 for site A and 0.98 for site B. A linear trend is seen before January with phase tapering off in the latter half of January in all the cases, which was expected from the snow depth measurements. It is also seen that the phase change is higher for 367 MHz data than that from the 262 MHz data. This is because phase change is directly proportional to frequency as shown in Eq. (3) and therefore with higher frequency we expect a larger phase change due to the change in SWE.

The SoOp receivers also collect data during the summer (i.e. snow free conditions) which is being used to develop the algorithm for extraction of reflectivity from the data for the purposes of RZSM retrieval. For examination of reflectivity, the power (as opposed to phase) of the reflected signal data with reference to the direct signal data is being examined. Figure 9 (right panel) shows a preliminary comparison between the *in-situ* measurement from averaged soil moisture probes from 5, 10, 27, and 40 cm and the measured reflection coefficient magnitude from data collected at the site with no vegetation from 367 MHz signal during June – July 2016, daily at 12 PM UTC. The correlation coefficient was 0.87. Furthermore, Figure 9 (left panel) shows the trend in the reflection coefficient magnitude that is observed at both sites. It can be seen that they follow each other very well (correlation coefficient 0.86).

SUMMARY

The HydroCube concept based on the P-band SoOp is proposed to provide cost-effective global sampling of RZSM and SWE to provide critical datasets for weather and climate forecasting, runoff prediction and water resource management, and prediction of flooding. The achievable spatial resolution is about 1-3 km and thus would allow the diagnostics of the spatial representation of the SWE and RZSM in global and regional land surface models. Because the spatial resolution is achieved by the coherent Fresnel reflection, the baseline antenna size is very small, about 30cmx30cm, significantly smaller than the ~10m size required for P-band synthetic aperture radars. The signal detection technologies would be the same as that used for the CYGNSS mission, providing the delay and Doppler shift of the reflected signal. The resulting satellite configuration could be implemented by small 6U satellites, leading to significant low cost for build and operation.

ACKNOWLEDGEMENT

The work described in this paper was carried out by the Jet Propulsion Laboratory, California Institute of Technology under a contract with the National Aeronautics and Space Administration.

REFERENCES

- [1] Chang, A.T.C., J. Foster, and D. Hall, "Nimbus-7 SMMR derived global snow cover parameters," *Ann. Glaciol.*, vol. 9, pp. 39–44, 1987.
- [2] Hallikainen, M., and P. Jolma (1992), Comparison of algorithms for retrieval of snow water equivalent from Nimbus-7 SMMR data in Finland, *IEEE Trans. Geosci. Remote Sens.*, 30, 124–131.
- [3] Kelly, R., A. Chang, L. Tsang, and J. Foster (2003), A prototype AMSR-E global snow area and snow depth algorithm, *IEEE Trans. Geosci. Remote Sens.*, 41, 230–242.
- [4] Durand, M., and S. A. Margulis (2007), Correcting first-order errors in snow water equivalent estimates using a multifrequency, multiscale radiometric data assimilation scheme, *J. Geophys. Res.*, 112, D13121, doi:10.1029/2006JD008067.
- [5] Entekhabi, D., E. G. Njoku, P. E. O'Neill, K. H. Kellogg, W. T. Crow, W. N. Edelstein, J. K. Entin, S. D. Goodman, T. J. Jackson, J. Johnson, J. Kimball, J. R. Piepmeier, R. D. Koster, N. Martin, K. C. McDonald, M. Moghaddam, S. Moran, R. Reichle, J. C. Shi, M. W. Spencer, S. W. Thurman, L. Tsang, and J. Van Zyl, The Soil Moisture Active Passive (SMAP) Mission, Proceedings of IEEE, Vol. 98, No. 5, pp. 704-716, May 2010.
- [6] Entekhabi, D., M. Moghaddam, "Mapping recharge from space: roadmap to meeting the grand challenge," *Hydrogeology Journal*, (2007) 15: 105-116.
- [7] Viviroli, D., H. H. Dürr, B. Messerli, M. Meybeck, and R. Weingartner, 2007, Mountains of the world, water towers for humanity: Typology, mapping, and global significance, *Water Resour. Res.*, 43, W07447, doi:10.1029/2006WR005653.
- [8] Koster, R. D., S. P. P. Mahanama, B. Livneh, D. P. Lettenmaier, and R. H. Reichle, 2010: Skill in streamflow forecasts derived from large-scale estimates of soil moisture and snow. *Nat. Geosci.*, 3, 613–616.
- [9] Mahanama, S., B. Livneh, R. Koster, D. Lettenmaier, and R. Reichle, 2012: Soil Moisture, Snow, and Seasonal Streamflow Forecasts in the United States. *J. Hydrometeorol.*, 13, 189–203, <https://doi.org/10.1175/JHM-D-11-046.1>
- [10] Ruf, C.S. S. Gleason, Z. Jelenak, S. Katzberg, A. Ridley, R. Rose, J. Scherrer, V. Zavorotny, IEEE Proc. Geoscience and Remote Sensing Symposium, 22-27 July 2012, Munich, Germany.
- [11] Katzberg, S., O. Torres, M. S. Grant, and D. Masters, "Utilizing calibrated GPS reflected signals to estimate soil moisture reflectivity and dielectric constant: Results from SMEX02," *Remote Sens. Environment*, 100 (2005), pp. 17-28.
- [12] Egido, A., S. Paloscia, E. Motte, L. Guerriero, N. Pierdicca, M. Caparrini, E. Santi, G. Fontanelli, N. Floury, "Airborne GNSS-R Polarimetric Measurement for Soil Moisture and Above Ground Biomass Estimation," *IEEE J. Selected Topics in Applied Earth Observations and Remote Sens.*, Vol. 7, No. 5, pp. 1522-1532, May 2014.
- [13] Zavorotny, V., K. Larsen, J. Braun, E. Small, E. Gutmann, A. Bilich, "A Physical Model for GPS Multipath Caused by Land Reflections: Toward Bare Soil Moisture Retrievals," *IEEE J. Selected Topics in Applied Earth Observations and Remote Sens.*, Vol. 3, Issue 1, pp. 100-110, March 2010, doi: 10.1109/JSTARS.2009.2033608
- [14] Shah, R., Garrison, J. L., Grant, M.S., Katzberg, S.J. and Tian, G., "Demonstration of Bistatic Radar for Ocean Remote Sensing using Communication Satellite Signals," *IEEE Geoscience and Remote Sensing Letters*, Vol. 9, No. 4, July, 2012, pp 619-623, doi:10.1109/LGRS.2011.2177061
- [15] Oetting, J. D., and T. Jen. "The mobile user objective system." *Johns Hopkins Apl Technical Digest* 30, no. 2 (2011): 103-112. (<http://techdigest.jhuapl.edu/TD/td3002/Oetting.pdf>)
- [16] Xu, X., S. Yueh, R. Shah, J. Garrison, A. Komanduru, and K. Elder, "Multi-frequency Reflectometry for Terrestrial Snow Cover Using Signals Of Opportunity, Proc. IEEE Geoscience and Remote Sensing Symposium, Milan Italy, 2015.
- [17] Yueh, S., X. Xu, R. Shah, Y. Kim, J. Garrison, A. Komanduru, and K. Elder Remote Sensing of Snow Water Equivalent Using Radio Signals of Opportunity: Theoretical Modeling, submitted to *IEEE Journal of Selected Topics in Applied Earth Observations and Remote Sensing*, 2016. (*Under Review*).
- [18] Shah, R., X. Xu, S. Yueh, C.-S. Chae, K. Elder, R. Starr, and Y. Kim, Remote Sensing of Snow Water Equivalent using P-band Coherent Detection, *IEEE Geosci. Remote Letts.*, Vol. 14, No. 3, pp. 309-313, March 2017.
- [19] Hallikainen, M. T., F. T. Ulaby, and T. E. Van Deventer, "Extinction Behavior of Dry Snow in the 18-to 90-GHz Range," *IEEE Transactions on Geoscience and Remote Sensing*, vol. GE-25, pp. 737-745, 1987.
- [20] Wiesmann, A., and C. Matzler, "Microwave Emission Model of Layered Snowpacks," *Remote Sens. Environ.*, 70, 307-316, 1999.
- [21] Rott, H., T. Nagler, and R. Scheiber, "Snow mass retrieval by means of SAR Interferometry," Proceedings of the FRINGE2003 Workshop, ESA/ESRIN, Frascati, Italy, ESA SP-550 (2004), 2004.

- [22] Leinss, S., A. Wiesmann, J. Lemmetyinen, and I. Hajnsek I (2015) Snow Water Equivalent of Dry Snow Measured by Differential Interferometry. *Selected Topics in Applied Earth Observations and Remote Sensing, IEEE Journal of* 8(8):3773-3790.
- [23] Tsang, L., J. A. Kong, and R. T. Shin, Theory of Microwave Remote Sensing, John Wiley & Sons, New York, 1985.
- [24] Chukhlantsev, A. J., A. M. Shutko, and S. P. Golovachev, Attenuation of Electromagnetic Waves by Vegetation Canopies in the 100-10000 MHz Frequency Band, <http://jre.cplire.ru/iso/feb03/4/text.html>
- [25] Mironov, V. L., L. G. Kosolapova, and S. V. Fomin, "Physically and mineralogically based spectroscopic dielectric model for moist soils," *IEEE Trans. Geosci. Remote Sens.*, 47(7), pp. 2059–2070, 2009.